Molecular g-Values, Magnetic Susceptibility Anisotropies, Second Moments of the Electronic Charge Distribution, Molecular Electric Quadrupole Moment, and ^{14}N Nuclear Quadrupole Coupling of Nitroethylene, $CH_2=CH-NO_2$

J. Spiekermann and D. H. Sutter

Abteilung Chemische Physik im Institut für Physikalische Chemie der Christian-Albrechts-Universität zu Kiel, Kiel, Germany

The high-field linear and quadratic Zeeman effect has been observed in nitroethylene. The spectrum is complicated by the presence of ^{14}N nuclear quadrupole coupling which was reanalyzed from low-J zero-field transitions observed under high resolution. Our ^{14}N quadrupole coupling constants are $X_{aa} = -0.8887(18)$ MHz, $X_{bb} = +0.0429(29)$ MHz, $X_{cc} = +0.8458(29)$ MHz (c-axis perpendicular to the molecular plane). Our g-values and magnetic susceptibility anisotropies, fitted to the observed high-field Zeeman multiplets, are $g_{aa} = -0.15\,985(39)$, $g_{bb} = -0.07197(31)$, $g_{cc} = -0.01080(32)$, $2\xi_{aa} - \xi_{bb} - \xi_{cc} = +19.07(43) \cdot 10^{-6}$ erg $\cdot$ G$^{-2} \cdot$ mole^{-1} and $2\xi_{bb} - \xi_{cc} - \xi_{aa} = +29.67(53) \cdot 10^{-6}$ erg $\cdot$ G$^{-2} \cdot$ mole^{-1}. From them, the anisotropies in the second moments of the electronic charge distribution and the components of the molecular electric quadrupole moment with respect to the principal inertia axes system follow as $\langle a^2 \rangle - \langle b^2 \rangle = +36.55(7)$ Å^2, $\langle b^2 \rangle - \langle c^2 \rangle = +23.58(9)$ Å^2, $\langle c^2 \rangle - \langle a^2 \rangle = -60.14(8)$ Å^2, $Q_{aa} = -0.59(29)$ D $\cdot$ Å, $Q_{bb} = +0.07(36)$ D $\cdot$ Å, and $Q_{cc} = +0.52(46)$ D $\cdot$ Å. The ^{14}N quadrupole coupling constants, the anisotropies in the second electronic moments and the quadrupole moments are compared to the corresponding Hartree-Fock SCF values calculated with the Gaussian 88 program. The discrepancy between the experimental values and the ab initio values is considerably larger than found earlier in a similar investigation of a group of imines.

Introduction

The present investigation is the fourth in a sequence of rotational Zeeman effect studies of small nitro-compounds [1–3]. Primarily we were aiming at experimental information on the local magnetic susceptibility tensor of the nitro-group [4, 5]. But the present study also provides accurate experimental data for comparison with quantum chemical results, which should be interesting, since nitroethylene appears to be a molecule for which standard ab initio programs give results which are in poor agreement with experiment (see below). Our work is based on earlier zero-field studies of the Zürich group, where a complete substitution-structure has been obtained by microwave spectroscopy [6, 7]. For later reference we present their structure in Figure 1. The corresponding nuclear coordinates are given in Table 1.

Experimental

The sample was prepared by direct dehydratisation of commercially available β-nitroethanol which, together with P_2O_5, was cautiously heated under vacuum (1 mTorr) until the reaction started [8]:

$$HO-CH_2-CH_2-NO_2 \xrightarrow[-H_2O]{\Delta T,\ P_2O_5} CH_2=CH-NO_2 \ .$$
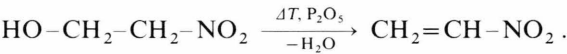
Table 1. Coordinates of the nuclei in nitroethylene (Ref. [7], Table 4, Fit 2). They result from an iterative least squares fit to the observed rotational constants of all singly substituted isotopic species and five multiply substituted isotopic species. a, b, and c refer to the principal axes system of the molecular moment of inertia tensor.

	a [Å]	b [Å]	c [Å]
C1	0.8066	0.6635	0.0000
C2	1.9390	−0.0234	0.0000
H1	0.6981	1.7377	0.0000
H2	2.8848	0.4920	0.0000
H3	1.9084	−1.1043	0.0000
N	−0.4827	−0.0170	0.0000
O1	−1.4729	0.7080	0.0000
O2	−0.5104	−1.2442	0.0000

Fig. 1. Microwave substitution structure of nitroethylene from [7], Table 4, fit 2. Also indicated are the deviations from sphericity in the second order contributions to the intramolecular Coulomb potential around the nitrogen nucleus and the corresponding β-axis of the nuclear quadrupole coupling tensor. Its α-axis is closely aligned to the N–C bond.

The sample was trapped in a cold trap and later purified in a sequence of vaccum distillations. Because of its reported tendency to polymerize under alkaline conditions, the glassware was rinsed with sulfuric acid prior to the preparation.

The spectra were recorded with our standard microwave Zeeman spectrometer [9] with 8.3 kHz square wave Stark effect modulation, which was operated in the X- through K-band region (8 to 26 GHz). Oversized brass waveguides were used as absorption cells with inner cross sections of 34 by 72 mm and 10 by 47 mm, respectively. The cells were cooled down to wall temperatures of about $-50\,°C$ by methanol flowing through cooling jackets.

Typical sample pressures were in the range of 0.5 to 1.0 mTorr. Due to the large dipole moment ($\mu_a = 3.51(2)$ D, $\mu_b = 1.16(8)$ D [6]) pressure broadening was predominant with experimental line widths in the range of 70 to 150 kHz (half-width at half hight). For the frequency determinations we have used a line shape analysis in which the molecular parameters on which the individual multiplet depends are directly fitted to the recorded spectrum. A more detailed description will be given in the subsequent section. In Figs. 2 and 3 we present typical recordings. A total of

ten low-J rotational transitions with J-values up to 3 were investigated, three of μ_a-type and seven of μ_b-type.

Theory and Analysis of the Spectra

A) Zero-field Spectra

Our analysis of the zero-field multiplets was based on the standard rigid rotor Hamiltonian including the quadrupole coupling of the ^{14}N nucleus. Spin-rotation coupling was estimated to contribute less than 1 kHz by the method described in [10] and was neglected.

Within this approximation the first order energy expression for the rotational states takes the following form [11]:

$$E_{J,K_a K_c,F}/h = B_a \cdot \langle \hat{J}_a^2 \rangle + B_b \cdot \langle \hat{J}_b^2 \rangle + B_c \cdot \langle \hat{J}_c^2 \rangle \qquad (1)$$

$$+ \frac{(3/4)\, C(C+1) - J(J+1)\, I(I+1)}{J(J+1)(2J+3)(2J-1)\, I(2I+1)}$$

$$\cdot \{ X_{aa} \cdot \langle \hat{J}_a^2 \rangle + X_{bb} \cdot \langle \hat{J}_b^2 \rangle + X_{cc} \cdot \langle \hat{J}_c^2 \rangle \}.$$

B_a, B_b, B_c Rotational constants,

J quantum number for the square of the rotational angular momentum,

Fig. 2. Zero field and Zeeman multiplets corresponding to the 101-000 rotational transition in nitroethylene. Within our approximate Hamiltonian the zero field splitting depends on the sum of the quadrupole coupling constants, $X_{bb} + X_{cc}$. In the Zeeman spectra the strong magnetic field has effectively uncoupled spin and overall rotation which leads to the observed doublet substructure with intensity ratio 2:1 corresponding to $M_I = \pm 1$ and $M_I = 0$ respectively. Within these doublets the splitting is due to the quadrupole coupling and carries no new information. In the Zeeman hfs pattern at right, which was observed under $\Delta M_J = \pm 1$ selection rule, the splitting between the two unresolved 'triplets' carries information on $g_{bb} + g_{cc}$.
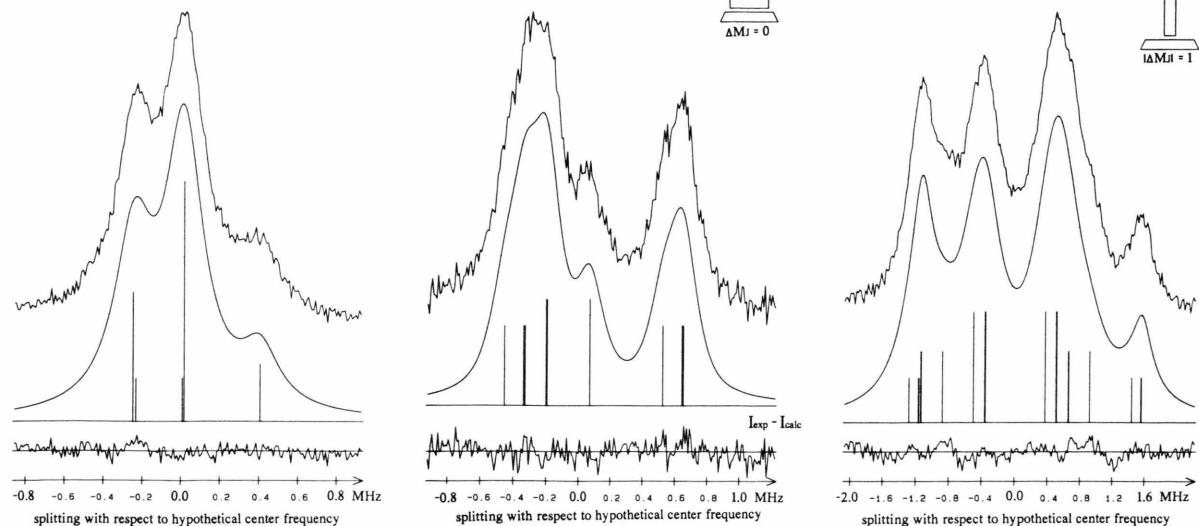

Fig. 3. Zero field and Zeeman multiplets corresponding to the 211-110 rotational transition. With the ^{14}N quadrupole coupling constants known from the zero field analysis, the $\Delta M_J = \pm 1$ Zeeman multiplet at right depends on the two independent susceptibility anisotropies $(2\,\xi_{aa} - \xi_{bb} - \xi_{cc})$, $(2\,\xi_{bb} - \xi_{cc} - \xi_{aa})$ and on two linear combinations of the g-values. These four parameters could be determined from the line profile with reasonable accuracy while a standard line profile analysis with all eighteen satellite frequencies as fitting parameters would have been unpractical.

K_a, K_c K-quantum numbers for the limiting pro-
late, K_a, and oblate, K_c, symmetric tops,

$\hat{J}_a, \hat{J}_b, \hat{J}_c$ operators corresponding to the compo-
nents of the rotational angular momen-
tum in direction of the principal inertia
axes measured in units of $h/2\pi$,

$\langle \hat{J}_g^2 \rangle$ indicates the asymmetric top expectation
value $\langle J, K_a K_c | \hat{J}_g^2 | J, K_a K_c \rangle$ $(g = a, b, c)$,

I spin quantum number for the ^{14}N nucleus,
i.e. $I = 1$.

$C = F(F+1) - J(J+1) - I(I+1)$ with F the quantum
number for the overall angular momen-
tum including spin and ranging from $|J - I|$
to $J + I$ in steps of one,

$X_{gg} = |e| Q \cdot \langle \partial^2 V / \partial g^2 \rangle / h$ quadrupole coupling con-
stants with e the electron charge, Q the
nuclear quadrupole moment of the ^{14}N
nucleus (close to 20 mbarn $= 2 \cdot 10^{-26}$ cm^2,
see below) and $\langle \partial^2 V / \partial g^2 \rangle$ $(g = a, b, c)$ the
vibronic expectation values of the second
derivatives of the intramolecular Coulomb
potential caused by the extranuclear charge
distribution and taken at the position of the
^{14}N nucleus.

Quite in general the numerical values for the funda-
mental constants were taken from Appendix D in [11].

The asymmetric top expectation values for the
squares of the angular momentum operators were cal-
culated as described as method b) on page 125 of [5].
The rotational constants determined earlier by the
Zürich group [6] were used as input in this calcula-
tion. Those $\langle \hat{J}_g^2 \rangle$-values, which are of relevance here,
are given in Table 2.

From Poisson's equation the sum of the second
derivatives of the Coulomb potential is zero, which
translates into

$$X_{aa} + X_{bb} + X_{cc} = 0 .$$

Thus the ^{14}N quadrupole hyperfine splittings (hfs)
depend on only two linear combinations of quadru-
pole coupling constants. Following common practice
we have chosen $X_+ = X_{bb} + X_{cc} = -X_{aa}$ and $X_- =
X_{bb} - X_{cc}$. Since most of the hfs-patterns could only
be partly resolved, we have used a two cycle line pro-
file analysis of the multiplets in order to extract X_+
and X_-.

In the first cycle a set of X_--values was preselected
ranging from $X_- = -0.765$ MHz to $X_- = -0.855$ MHz
with a step width of 15 kHz and for each hfs multiplet

Table 2. Asymmetric top expectation values for the squares
of the rotational momentum operators in the lowest rota-
tional states. They were calculated using the rotational con-
stants reported in [6], i.e. $B_a = 11811.757$ (10) MHz, $B_b =
4680.7851$ (21) MHz, and $B_c = 3353.7697$ (25) MHz.

J	K_a	K_c	$\langle J_a^2 \rangle$	$\langle J_b^2 \rangle$	$\langle J_c^2 \rangle$
0	0	0	0.000000	0.000000	0.000000
1	0	1	0.000000	1.000000	1.000000
1	1	1	1.000000	0.000000	1.000000
1	1	0	1.000000	1.000000	0.000000
2	0	2	0.021391	2.736660	3.241949
2	1	2	1.000000	1.000000	4.000000
2	1	1	1.000000	4.000000	1.000000
2	2	1	4.000000	1.000000	1.000000
2	2	0	3.978609	1.263340	0.758051
3	0	3	0.100567	4.737043	7.162390
3	1	3	1.011951	2.348923	8.639126
3	1	2	1.015414	8.316675	2.667911
3	2	2	4.000000	4.000000	4.000000
3	2	1	3.899433	5.262957	2.837610
3	3	1	8.988049	1.651077	1.360874
3	3	0	8.984586	1.683325	1.332089

X_+, the halfwidth, the hypothetical center frequency
and one intensity were least squares fitted to the ob-
served line profile. (The relative intensities of the hfs
satellites are known from theory.) For the line profiles
we have used the superposition of a Lorentzian and a
Gaussian line for the satellites with the intensity ratio
$I_{\text{Lorentzian}} / I_{\text{Gaussian}}$ as additional fitting parameter.
This procedure represents a practicable compromise
between pressure broadening ($\to$ Lorentzian) and
Doppler broadening ($\to$ Gaussian) on the one hand,
which, combined, would result in a Voigt-profile, and
modulation broadening on the other hand. Usually it
leads to a good reproduction of the observed line
profiles (compare also [12]). The Lorentzian contribu-
tion outweighed the Gaussian contribution by a ratio
typically in the order of 9:1.

The result is shown in Table 3. In general for each
multiplet a different optimal X_+-value, $X_{+\text{opt}}$, is ob-
tained that way. This reflects the fact that the pre-
selected X_--values are not the true values and that the
individual patterns are typically determined by a spe-
cial linear combination of the quadrupole coupling
constants. The 101–000 multiplet for instance de-
pends on $X_{bb} + X_{cc}$. These linear correlations between
X_- and $X_{+\text{opt}}$ are clearly visible from Table 3. Ideally
the linear correlations should intercept in a single
point. Noise and possibly minor deficiencies of the
model prevent this. But the mean deviations from
$X_{+\text{opt}}$ clearly go through a minimum, located some-
where in between the preselected values $X_- = -0.795$

Table 3. X_+-values (in MHz) fitted to the observed hfs-patterns with X_- fixed to -0.765 MHz, -0.780 MHz, etc. Since X_- and X_+ are practically correlated for each individual hfs-pattern, there is only little difference in the quality of these fits throughout the X_-, X_+-range covered in this table. For the correct X_--value all X_+-values should turn out equal. Noise and possibly deficiencies in the effective Hamiltonian prevent this, but the mean deviation in the X_+-values clearly goes through a minimum close to $X_- = -0.805$ MHz.

X_- [MHz]	−0.765	−0.780	−0.795	−0.810	−0.825	−0.840
101−000	0.8786	0.8786	0.8786	0.8786	0.8786	0.8786
110−101	0.9135	0.9077	0.9017	0.8956	0.8896	0.8830
202−101	0.9080	0.9080	0.9080	0.9080	0.9080	0.9079
211−110	0.9026	0.8921	0.8875	0.8829	0.8782	0.8735
212−111	0.8966	0.9019	0.9008	0.8994	0.8977	0.8958
220−211	0.8762	0.8884	0.8907	0.8929	0.8951	0.8973
221−212	0.8785	0.8735	0.8685	0.8635	0.8585	0.8535
202−111	0.8860	0.8788	0.8815	0.8842	0.8869	0.8896
312−303	0.9468	0.9255	0.9039	0.8820	0.8601	0.8382
average	0.8985	0.8949	0.8912	0.8875	0.8836	0.8797
mean dev.	0.0227	0.0172	0.0134	0.0131	0.0166	0.0221

MHz and $X_- = -0.810$ MHz. Therefore the same procedure was repeated for this narrower range with the step width for X_- reduced to 1 kHz, and the minimum mean deviation from $X_{+\,\mathrm{opt}}$ was found at $X_- = -0.805$ MHz.

Then, in a second cycle X_- was fixed to this value and again for each hfs-pattern X_+ was optimized for best reproduction of the observed line profile. Within our effective Hamiltonian each of these optimized X_+-values stands for the complete set of "experimental" hfs-satellites of the corresponding multiplet. In the last step these "experimental satellite frequencies", they are given in Table 4, were used as input data into our program AVB for the final fit, now of both quadrupole coupling parameters X_+ and X_-.

The result of this final fit of the quadrupole coupling constants was:

$$X_+ = X_{bb} + X_{cc} = +0.8887(18) \text{ MHz},$$
$$X_- = X_{bb} - X_{cc} = -0.8029(40) \text{ MHz}$$

or

$$X_{aa} = -0.8887(18) \text{ MHz},$$
$$X_{bb} = +0.0429(29) \text{ MHz},$$
$$X_{cc} = +0.8458(29) \text{ MHz}$$

(throughout this contribution uncertainties are single standard deviations).

Figures 2 and 3 give an impression of the good agreement between the observed multiplet profiles and those calculated from the final X_+ and X_- values. For comparison we quote the corresponding values determined earlier by the Zürich group [6]: $X_{aa} = -0.883(49)$ MHz, $X_{bb} = +0.014(24)$ MHz and $X_{cc} =$ $+0.869(49)$ MHz. The slight differences may be partly due to the fact that the Zürich results were derived in a simultaneous fit of the quadrupole coupling constants and the rotational constants. Also in the Zürich study only five hfs multiplets were used to fit the data. Below we will compare the observed quadrupole coupling constants to Hartree-Fock SCF results calculated at the substitution-structure.

B) Zeeman Spectra

For the analysis of the Zeeman multiplets, which were recorded under $\Delta M_J = 0$ and $\Delta M_J = \pm 1$ selection rules, the effective Hamiltonian was set up in the uncoupled asymmetric top basis and was diagonalized numerically. All matrix elements off-diagonal in the rigid rotor quantum numbers J and $K_a K_c$ were neglected. For the matrix elements we refer to Eqs. (2), (4), (5), and (6) of [3]. A line profile analysis similar to the one described above was carried out with the ^{14}N quadrupole coupling constants and center frequencies fixed to their values determined from the zero field multiplets and the g-values and susceptibility anisotropies as fitting parameters. Our experimental frequencies are listed in Table 5. The molecular g-values and magnetic susceptibility anisotropies, which were fitted to the observed splittings, are

$$g_{aa} = -0.15985(39),$$
$$g_{bb} = -0.07197(31),$$
$$g_{cc} = -0.01080(32),$$
$$2\xi_{aa} - \xi_{bb} - \xi_{cc} = +19.07(43) \cdot 10^{-6} \text{ erg} \cdot \text{G}^{-2} \cdot \text{mol}^{-1},$$
$$2\xi_{bb} - \xi_{cc} - \xi_{aa} = +29.67(53) \cdot 10^{-6} \text{ erg} \cdot \text{G}^{-2} \cdot \text{mol}^{-1}.$$

Table 4. Zero field ^{14}N-hfs-satellite frequencies fitted to the observed line profiles as described in the text.

$J'\,K'_a\,K'_c - J\,K_a\,K_c$ v_c(exp) [MHz]	$F'-F$	Rel. Int.	Δv(exp) [MHz]	Δv(cal) [MHz]	Δv(exp) $-\Delta v$(cal) [MHz]
1 0 1 − 0 0 0	2 − 1	55.5	0.0439	0.0444	−0.0005
8034.5609	1 − 1	33.3	−0.2196	−0.2222	0.0026
	0 − 1	11.1	0.4393	0.4443	−0.0050
1 1 0 − 1 0 1	2 − 2	41.7	−0.0874	−0.0867	−0.0007
8458.0016	1 − 1	8.33	0.4372	0.4336	0.0036
	1 − 2	13.9	0.1680	0.1670	0.0010
	0 − 1	11.1	−0.2012	−0.2007	−0.0005
	2 − 1	13.9	0.1818	0.1799	0.0019
	1 − 0	11.1	−0.2360	−0.2329	−0.0031
2 0 2 − 1 0 1	3 − 2	46.6	0.0236	0.0232	0.0004
15900.5706	2 − 1	25.0	−0.0145	−0.0145	0.0000
	1 − 0	11.1	−0.2125	−0.2076	−0.0049
	2 − 2	8.33	−0.2869	−0.2804	−0.0065
	1 − 1	8.33	0.4685	0.4589	0.0096
2 1 1 − 1 1 0	3 − 2	46.6	0.0450	0.0454	−0.0004
17396.0973	2 − 1	25.0	−0.2211	−0.2222	0.0011
	1 − 0	11.1	0.4323	0.4336	−0.0013
	2 − 2	8.33	0.0323	0.0316	0.0007
	1 − 1	8.33	−0.2013	−0.2007	−0.0006
2 1 2 − 1 1 1	3 − 2	46.6	0.0634	0.0626	0.0008
14742.0578	2 − 1	25.0	−0.2256	−0.2222	−0.0034
	1 − 0	11.1	0.2377	0.2329	0.0048
	2 − 2	8.33	−0.2110	−0.2093	−0.0017
	1 − 1	8.33	0.2012	0.2007	0.0005
2 2 0 − 2 1 1	3 − 3	41.5	−0.0710	−0.0707	−0.0003
21561.3688	2 − 2	23.1	0.2485	0.2474	0.0011
	1 − 1	15.0	−0.2485	−0.2474	−0.0011
	2 − 3	5.19	0.2345	0.2336	0.0009
	1 − 2	5.00	−0.2267	−0.2260	−0.0007
	3 − 2	5.19	−0.0569	−0.0569	0.0000
	2 − 1	5.00	0.2268	0.2260	0.0008
2 2 1 − 2 1 2	3 − 3	41.5	−0.1215	−0.1239	0.0024
25373.8938	2 − 2	23.1	−0.4251	0.4336	−0.0085
	1 − 1	15.0	−0.4251	−0.4336	0.0085
	2 − 3	5.19	0.1566	0.1618	−0.0052
	1 − 2	5.00	−0.0075	−0.0107	0.0032
	3 − 2	5.19	0.1470	0.1480	−0.0010
	2 − 1	5.00	0.0075	0.0107	−0.0032
2 0 2 − 1 1 1	3 − 2	46.6	0.0693	0.0699	−0.0006
8769.6118	2 − 1	25.0	−0.2451	−0.2473	0.0022
	1 − 0	11.1	0.2551	0.2582	−0.0031
	2 − 2	8.33	−0.2334	−0.2344	0.0010
	1 − 1	8.33	0.2257	0.2261	−0.0004
3 0 3 − 3 1 2	4 4	40.2	−0.0621	−0.0620	−0.0001
12487.9732	3 3	28.0	0.1862	0.1859	0.0003
	2 2	21.2	−0.1490	−0.1487	−0.0003
	4 3	2.68	−0.1570	−0.1570	0.0000
	3 2	2.65	0.3143	0.3142	0.0001
	3 4	2.68	0.2811	0.2809	0.0002
	2 3	2.65	−0.2771	−0.2770	−0.0001

Table 5. Center frequencies, v_c, and Zeeman splittings, $\Delta v = v - v_c$, from the line profile analysis described in the text. The $\Delta M_J = 0$ pattern of the 211−110 transition was partly perturbed by a yet unassigned spectral feature. The corresponding satellites (*) were omitted. Low-intensity satellites, put into brackets, were not included in the fit.

$J' K'_a K'_c - J K_a K_c$ v_c(exp) [MHz] H ΔM_J	M_I	$M'_J - M_J$	Rel. Int.	Δv(exp) [MHz]	Δv(cal) [MHz]	Δv(exp) $-\Delta v$(cal) [MHz]
1 0 1 − 0 0 0 8034.5609 15653G, 0	−1	0 − 0	2	−0.1628	−0.1635	0.0007
	0	0 − 0	2	0.1003	0.0997	0.0006
	1	0 − 0	2	−0.1697	−0.1702	0.0005
1 1 0 − 1 0 1 8458.0016 13138G, 0	−1	−1 − −1	2	−0.9259	−0.9309	0.0050
	−1	1 − 1	2	0.5635	0.5592	0.0043
	0	−1 − −1	2	−0.6651	−0.6696	0.0045
	0	1 − 1	2	0.8248	0.8214	0.0034
	1	−1 − −1	2	−0.9246	−0.9282	0.0036
	1	1 − 1	2	0.5649	0.5619	0.0030
1 1 0 − 1 0 1 8458.0016 15653G, 0	−1	−1 − −1	2	−1.1091	−1.1148	0.0057
	−1	1 − 1	2	0.6733	0.6615	0.0118
	0	−1 − −1	2	−0.8484	−0.8536	0.0052
	0	1 − 1	2	0.9344	0.9234	0.0110
	1	−1 − −1	2	−1.1080	−1.1124	0.0044
	1	1 − 1	2	0.6744	0.6637	0.0107
2 1 1 − 1 1 0 17396.0973 15653G, 0	−1	−1 − −1	6	0.6490	0.6551	−0.0061
	−1	0 − 0	8	−0.1969	−0.2029	0.0060
	−1	1 − 1	6	*	−0.2951	*
	0	−1 − −1	6	0.5296	0.5353	−0.0057
	0	0 − 0	8	0.0689	0.0627	0.0062
	0	1 − 1	6	*	−0.4123	*
	1	−1 − −1	6	0.6578	0.6628	−0.0050
	1	0 − 0	8	−0.1911	−0.1977	0.0066
	1	1 − 1	6	*	−0.2873	*
2 1 2 − 1 1 1 14742.0578 15653G, 0	−1	−1 − −1	6	0.3190	0.3143	0.0047
	−1	0 − 0	8	−0.0862	−0.0831	−0.0031
	−1	1 − 1	6	−0.6387	−0.6277	−0.0110
	0	−1 − −1	6	0.4028	0.3980	0.0048
	0	0 − 0	8	0.1105	0.1083	0.0022
	0	1 − 1	6	−0.5606	−0.5495	−0.0111
	1	−1 − −1	6	0.3124	0.3076	0.0048
	1	0 − 0	8	−0.0860	−0.0882	0.0022
	1	1 − 1	6	−0.6453	−0.6342	−0.0111
1 0 1 − 0 0 0 8034.5609 15633G, ±1	−1	−1 − 0	1	−0.4058	−0.4098	0.0040
	−1	1 − 0	1	0.5734	0.5866	−0.0132
	0	−1 − 0	1	−0.5426	−0.5465	0.0039
	0	1 − 0	1	0.4331	0.4465	−0.0134
	1	−1 − 0	1	−0.4161	−0.4198	0.0037
	1	1 − 0	1	0.5631	0.5765	−0.0134
1 0 1 − 1 0 1 8458.0016 15633G, ±1	−1	−1 − 0	1	0.6928	0.6959	−0.0031
	−1	0 − −1	1	−1.3545	−1.3598	0.0053
	−1	0 − 1	1	1.4127	1.4107	0.0020
	−1	1 − 0	1	−0.2931	−0.3005	−0.0074
	0	−1 − 0	1	0.5733	0.5762	−0.0029
	0	0 − −1	1	−1.4931	−1.4985	0.0054
	0	0 − 1	1	1.2714	1.2692	0.0022
	0	1 − 0	1	−0.4090	−0.4168	0.0078
	1	−1 − 0	1	0.6981	0.7007	−0.0026
	1	0 − −1	1	−1.3552	−1.3608	0.0056
	1	0 − 1	1	1.4118	1.4095	0.0023
	1	1 − 0	1	−0.2877	−0.2957	0.0080
2 1 1 − 1 1 0 17396.0973 15633G, ±1	−1	−2 − −1	6	−0.3745	−0.3818	0.0073
	−1	0 − −1	1	(1.6341)	1.6066	0.0275
	−1	−1 − 0	3	−1.1745	−1.1550	−0.0195
	−1	1 − 0	3	0.6667	0.6664	0.0003
	−1	0 − 1	1	(−1.1813)	−1.1639	−0.0174
	−1	2 − 1	6	0.4929	0.4906	0.0023
	0	−2 − −1	6	−0.5081	−0.5154	0.0073
	0	0 − −1	1	(1.5189)	1.4914	0.0275
	0	−1 − 0	3	−0.9135	−0.8941	−0.0194
	0	1 − 0	3	0.9276	0.9273	0.0003
	0	0 − 1	1	(−1.2938)	−1.2764	−0.0174
	0	2 − 1	6	0.3616	0.3597	0.0019
	1	−2 − −1	6	−0.3667	−0.3741	0.0074
	1	0 − −1	1	(1.6419)	1.6143	0.0276
	1	−1 − 0	3	−1.1693	−1.1499	−0.0195
	1	1 − 0	3	0.6719	0.6716	0.0003
	1	0 − 1	1	(−1.1734)	−1.1560	−0.0174
	1	2 − 1	6	0.5004	0.4985	0.0019
2 1 2 − 1 1 1 14742.0578 15633G, ±1	−1	−2 − −1	6	0.0543	0.0685	−0.0142
	−1	0 − −1	1	(0.7195)	0.7584	−0.0389
	−1	−1 − 0	3	−0.5191	−0.5275	0.0084
	−1	1 − 0	3	0.5561	0.5653	−0.0092
	−1	0 − 1	1	(−1.2445)	−1.2751	0.0306
	−1	2 − 1	6	0.2447	0.2247	0.0200
	0	−2 − −1	6	−0.1366	−0.1223	−0.0143
	0	0 − −1	1	(0.8916)	0.9306	−0.0390
	0	−1 − 0	3	−0.4160	−0.4245	0.0085
	0	1 − 0	3	0.6535	0.6628	−0.0093
	0	0 − 1	1	(−1.0723)	−1.1030	0.0303
	0	2 − 1	6	0.0551	0.0351	0.0200
	1	−2 − −1	6	0.0490	0.0632	−0.0142
	1	0 − −1	1	(0.7143)	0.7533	−0.0390
	1	−1 − 0	3	−0.5258	−0.5342	0.0084
	1	1 − 0	3	0.5495	0.5588	−0.0093
	1	0 − 1	1	(−1.2496)	−1.2802	0.0306
	1	2 − 1	6	0.2397	0.2198	0.0199

In principle a second set of g-values, all signs reversed, would fit the high-field Zeeman spectra equally well (compare [5], p. 145). Since it would lead to unreasonable values for the molecular electric quadrupole moments and individual components of the magnetic susceptibility tensor (see below), it could be discarded.

Derived Molecular Parameters

The results of a rotational Zeeman effect study can be used to derive experimental values for other electronic ground state expectation values such as the molecular electric quadrupole moments and the anisotropies in the electronic second moments. This derivation is based on the theoretical expressions for the elements of the molecular g-tensor and of the magnetic susceptibility tensor.

The theoretical expressions for the molecular g-tensor elements have been given by Wick [13] and Eshbach and Strandberg [14]. Those for the magnetic susceptibilities have been given by Van Vleck [15]. An unified theoretical derivation for both tensors, which starts from the Lagrangian of the molecule rotating in an exterior magnetic field has been presented by Sutter

$$\xi_{aa} = -N \frac{e^2}{4mc^2} \left\{ \langle 0 | \sum_{\varepsilon}^{\text{electrons}} (b_\varepsilon^2 + c_\varepsilon^2) | 0 \rangle + 2/m \sum_{n}^{\text{ex. states}} \frac{|\langle n | \hat{L}_a | 0 \rangle|^2}{E_0 - E_n} \right\} \quad (3)$$

(and cyclic permutations),

N Avogadro's number,
h Planck's constant,
m_p proton mass,
Z_v atomic number of the v-th nucleus,
a_v, b_v, c_v coordinates of the v-th nucleus with respect to the molecular principal inertia axes system,
$a_\varepsilon, b_\varepsilon, c_\varepsilon$ coordinates of the ε-th electron,
m electron mass,
e electron charge,
$\hat{L}_a = \hbar/i \sum (b_\varepsilon \partial/\partial c_\varepsilon - c_\varepsilon \partial/\partial b_\varepsilon)$ component of the electronic angular momentum operator.

The brackets $\langle \ldots \rangle$ indicate electronic matrix elements. The perturbation sum runs over the excited electronic states.

By rearranging terms, Hüttner, Lo, and Flygare [16] have related these Zeeman parameters to the molecular electronic quadrupole moments and to the anisotropies in the electronic second moments:

$$Q_{aa} = \frac{1}{2} |e| \left\{ \sum_{v}^{\text{nuclei}} Z_v (2a_v^2 - b_v^2 - c_v^2) - \langle 0 | \sum_{\varepsilon}^{\text{electrons}} (2a_\varepsilon^2 - b_\varepsilon^2 - c_\varepsilon^2) | 0 \rangle \right\}$$

$$= -\frac{h|e|}{16\pi^2 m_p} \left(\frac{2g_{aa}}{B_a} - \frac{g_{bb}}{B_b} - \frac{g_{cc}}{B_c} \right) - \frac{2mc^2}{|e|N} (2\xi_{aa} - \xi_{bb} - \xi_{cc}), \quad (4)$$

$$\langle 0 | \sum (a_\varepsilon^2 - b_\varepsilon^2) | 0 \rangle = \sum_{v}^{\text{nuclei}} Z_v (a_v^2 - b_v^2) + \frac{h}{8\pi^2 m_p} \left(\frac{g_{aa}}{B_a} - \frac{g_{bb}}{B_b} \right) + \frac{4mc^2}{3e^2 N} \{ (2\xi_{aa} - \xi_{bb} - \xi_{cc}) - (2\xi_{bb} - \xi_{cc} - \xi_{aa}) \} \quad (5)$$

(and cyclic permutations).

The individual components of the electronic second moments follow as

$$\langle 0 | \sum a_\varepsilon^2 | 0 \rangle = \frac{2mc^2}{Ne^2} (\xi_{aa} - \xi_{bb} - \xi_{cc}) + \frac{h}{16\pi^2 m_p} \left(\frac{g_{aa}}{B_a} - \frac{g_{bb}}{B_b} - \frac{g_{cc}}{B_c} \right) + \sum_{v}^{\text{nuclei}} Z_v a_v^2 \quad (6)$$

(and cyclic permutations).

and Flygare [5]. For convenience of the reader we present the expressions for the g- and ξ-elements:

$$g_{aa} = \frac{8\pi^2 m_p B_a}{h} \left\{ \sum_{v}^{\text{nuclei}} Z_v (b_v^2 + c_v^2) + 2/m \sum_{n}^{\text{ex. states}} \frac{|\langle n | \hat{L}_a | 0 \rangle|^2}{E_0 - E_n} \right\}, \quad (2)$$

Note that different definitions exist in the literature for the quadrupole moments, and that in the definition used here all quantities are referred to the principal inertia axes system. Since the experimental g-values, rotational constants and susceptibility anisotropies, which enter into the expressions for the quadrupole moments, correspond to vibronic ground state exceptation values, also the quadrupole moments derived

according to (4) will come close to vibronic ground state expectation values (see [5], p. 104).

We note that, if the electron density would be a superposition of spherical (atomic) charge distributions, the second moments could be written as

$$\langle g^2 \rangle = \sum_v^{\text{nuclei}} Z_v g_v^2 + k_H \cdot n_H + k_C \cdot n_C + k_N \cdot n_N + k_O \cdot n_O$$
$$(g = a, b, c),$$

where n_H, n_C, n_N, and n_O are the numbers of H-, C-, N-, and O-atoms in the molecule and where k_H, k_C, k_N, and k_O are constants. (Flygare and coworkers have proposed to use $k_H = 0.25$ and $k_C = k_N = k_O = 1.00$ for rule of thumb predictions [17].)

Within this "superposition of spherical charges" approach, the molecular electric quadrupole moments would be zero and the anisotropies in the second electronic moments would equal the corresponding anisotropies in the nuclear charge distribution e.g.

$$\langle a^2 \rangle - \langle b^2 \rangle = \sum_v^{\text{nuclei}} Z_v a_v^2 - \sum_v^{\text{nuclei}} Z_v b_v^2 \text{ etc. Thus the}$$

changes in the electronic charge distribution, which occur upon bond formation, are directly reflected in the molecular quadrupole moments but only change the trailing digits in the second electronic moments and their anisotropies.

We present our derived molecular parameters in Table 6. They will be compared to quantum chemical results in the final section.

The sums

$$\sum_v^{\text{nuclei}} Z_v a_v^2 = 59.984(18)\ \text{Å}^2,$$

$$\sum_v^{\text{nuclei}} Z_v b_v^2 = 23.522(12)\ \text{Å}^2,$$

$$\sum_v^{\text{nuclei}} Z_v c_v^2 = 0.000\ \text{Å}^2,$$

including their uncertainties, which enter into the anisotropies of the electronic second moments were calculated from the substitution-structure given in Table 1.

In the lower part of Table 6 several less accurate data are included. Their derivation is based on an estimate of the out of plane second electronic moment, $\langle \sum_\varepsilon^{\text{electrons}} c_\varepsilon^2 \rangle$, as additional input. For this estimate we have used the rule of thumb (see above), i.e. $1\ \text{Å}^2$ for every in-plane heavy atom (C, N, and O) and $0.25\ \text{Å}^2$ for every in-plane hydrogen. This leads to $\langle 0 | \sum_v^{\text{electrons}} c_\varepsilon^2 | 0 \rangle = 5.75\ \text{Å}^2$. For error propagation we have assumed an uncertainty of $0.25\ \text{Å}^2$ in this value.

Depending on the choice of sign for the g-values, two sets of derived parameters are obtained. The set based on positive g-values can be discarded because it leads to unreasonably large absolute values for the molecular quadrupole moments and susceptibilities.

Table 6. Molecular quantities, derived from the g-values, susceptibility anisotropies, rotational constants, and nuclear coordinates of nitroethylene. (a) With $\sum Z_v a_v^2$ and $\sum Z_v b_v^2$ as additional input, (b) with $\langle \sum c^2 \rangle = 5.75\ (25)\ \text{Å}^2$ from the rule of thumb as additional input (see text).

		Negative g-values	Positive g-values
Molecular electric quadrupole moments $[10^{-26}\ \text{esu} \cdot \text{cm}^2]$	$\begin{cases} Q_{aa} \\ Q_{bb} \\ Q_{cc} \end{cases}$	$-0.59\ (29)$ $0.07\ (36)$ $0.52\ (46)$	$-21.00\ (29)$ $-33.66\ (36)$ $54.67\ (46)$
Anisotropies in the second electronic moments [Å] (a)	$\begin{cases} \langle \Sigma(a^2-b^2)\rangle \\ \langle \Sigma(b^2-c^2)\rangle \\ \langle \Sigma(c^2-a^2)\rangle \end{cases}$	$36.55\ (7)$ $23.58\ (9)$ $-60.14\ (8)$	$34.70\ (7)$ $35.78\ (9)$ $-70.49\ (8)$
Bulk susceptibility $[10^{-6}\ \text{erg} \cdot \text{G}^{-2} \cdot \text{mol}^{-1}]$ (b)	ξ_{bulk}	$-26.60\ (219)$	$-135.96\ (219)$
Diagonal elements of susceptibility tensor $[10^{-6}\ \text{erg} \cdot \text{G}^{-2} \cdot \text{mol}^{-1}]$ (b)	$\begin{cases} \xi_{aa} \\ \xi_{bb} \\ \xi_{cc} \end{cases}$	$-20.25\ (219)$ $-16.71\ (220)$ $-42.85\ (220)$	$-129.60\ (219)$ $-126.07\ (220)$ $-152.21\ (220)$
Second electronic moments $[\text{Å}^2]$ (b)	$\begin{cases} \langle \Sigma a^2 \rangle \\ \langle \Sigma b^2 \rangle \\ (\langle \Sigma c^2 \rangle) \end{cases}$	$65.89\ (26)$ $29.33\ (26)$ $5.75\ (25)$	$76.24\ (26)$ $41.53\ (26)$ $5.75\ (25)$

Table 7. Prediction of the bulk susceptibility of nitroethylene (in units of 10^{-6} erg $\cdot$ G^{-2} $\cdot$ mol^{-1}) from the experimental value for nitrobenzene [19] using Haberditzl's additivity scheme for core and bond contributions (see p. 96–97 of [18]).

Bulk susceptibility nitrobenzene:		−61.8
−4 H cores	(0.0 each)	0.0
−4 C cores	(−0.15 each)	+ 0.6
−4 C–H σ-bonds	(−3.2 each)	+12.8
−5 C–C σ-bonds	(−2.4 each)	+12.0
−2 C–C π-bonds	(−2.2 each)	+ 4.4
− 'ring current'	(−13.7)	+13.7
H–C=C–NO$_2$ intermediate		−18.3
+2 H cores	(0.0 each)	0.0
+1 HC–H σ-bond	(−3.6 each)	−3.6
+1 C–H σ-bond	(−3.2 each)	−3.2
Bulk susceptibility nitroethylene:		−25.1

We demonstrate this in the case of the bulk susceptibility. For it, a reasonable value can be estimated also along a different route within Haberditzl's additivity scheme for core and bond contributions [18]. Starting point is the experimental value for the bulk susceptibility of nitrobenzene, ξ_{bulk}(C$_6$H$_5$NO$_2$) $= -61.8 \cdot 10^{-6}$ erg $\cdot$ G^{-2} $\cdot$ mole^{-1} [19]. By subtraction of the appropriate core-, bond- and π-ring-current increments as compiled in Table 7, one obtains ξ_{bulk}(CH$_2$=CHNO$_2$) $= -25.1 \cdot 10^{-6}$ erg $\cdot$ G^{-2} $\cdot$ mole^{-1}. This is close to the value predicted from our $\langle c^2 \rangle$-estimate and negative g-values, but it is far off the value which would follow if the signs of the g-values were positive. In the final section of our paper we will compare also the molecular quadrupole moments and anisotropies in the electronic second moments to the corresponding ab initio values.

Comparison with Related Molecules and with ab initio Results

We subdivide this section into three parts. First we compare our experimental ^{14}N quadrupole coupling constants with the corresponding values observed in nitromethane [20] and nitrobenzene [21]. Second we compare them with the results from restricted Hartree-Fock self consistent field calculations (RHF-SCF) carried out with basis sets of different quality. Third we turn to the second moments of the molecular charge distribution, i.e. we compare the experimental values for the molecular electric quadrupole moments, Q_{aa} etc., the anisotropies in the electronic second moments, $\langle 0 | \sum (a_\varepsilon^2 - b_\varepsilon^2) | 0 \rangle$ etc., and the electronic sec-

Table 8. Comparison between the experimental values for the ^{14}N nuclear quadrupole coupling constants with those reported for nitromethane [20] and nitrobenzene [21]. In nitromethane and in nitrobenzene the principal axes of the coupling tensor are parallel to the principal axes of the molecular moment of inertia tensor with the a- and α-axes parallel to the C–N bond and the c- and γ-axes perpendicular to the NO$_2$-plane. For nitroethylene we give three sets of 'experimental' values. Those marked by [a] were calculated from the experimental values assuming $\delta = \sphericalangle (\alpha, a) = 27.83°$, those marked by [b] were calculated using $\delta = 26.25°$ and those marked by [c] follow from $\delta = 25.07°$ (see text).

Nitroethylene	$X_{\alpha\alpha}$ [MHz]	−1.248 [a]	−1.188 [b]	−1.150 [c]
	$X_{\beta\beta}$ [MHz]	0.402 [a]	0.342 [b]	0.304 [c]
	$X_{\gamma\gamma}$ [MHz]	0.846 [a]	0.846 [b]	0.846 [c]
Nitromethane	$X_{\alpha\alpha}$ [MHz]	−1.184 (7)		
	$X_{\beta\beta}$ [MHz]	0.305 (12)		
	$X_{\gamma\gamma}$ [MHz]	0.880 (12)		
Nitrobenzene	$X_{\alpha\alpha}$ [MHz]	−1.159 (3)		
	$X_{\beta\beta}$ [MHz]	0.304 (4)		
	$X_{\gamma\gamma}$ [MHz]	0.855 (4)		

ond moments themselves, $\langle 0 | \sum a_\varepsilon^2 | 0 \rangle$ etc., with the corresponding ab initio results.

The comparison of the ^{14}N nuclear quadrupole coupling constants of nitroethylene with those observed in nitromethane and nitrobenzene, two other nitro-compounds investigated by microwave spectroscopy, is presented in Table 8. Only the out of plane components, X_{cc}, can be compared directly, since in nitroethylene the principal axes of the ^{14}N quadrupole coupling tensor, α, β, are not aligned to the molecular principal inertia axes a, b (comp. Figure 1). For the determination of the coupling constants $X_{\alpha\alpha}$ and $X_{\beta\beta}$ also in nitroethylene, ($X_{\gamma\gamma} = X_{cc}$), the knowledge of X_{ab} or of $\delta = \sphericalangle (\alpha, a)$, the angle between the α- and a-axes, would be required. Unfortunately X_{ab} could not be determined in the present investigation. However, approximate values for $X_{\alpha\alpha}$ and $X_{\beta\beta}$ can be predicted if one assumes that the orientation of the ^{14}N quadrupole coupling tensor is given by the bonds. Intuitively one will try two choices:

a) Assume that the α-axis is aligned to the C–N bond. This leads to an angle $\delta = \sphericalangle(\alpha, a) = 27.83°$ (see structure).

b) Assume that the α-axis is aligned to the bisector of the O–N–O bond angle. This leads to an angle $\delta = 26.25°$ (see structure).
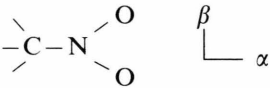
With δ assumed as above, $X_{\alpha\alpha}$ and $X_{\beta\beta}$ follow from X_{aa} and X_{bb} through the transformation

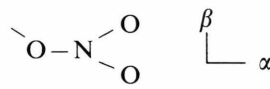$$X_{aa} = \cos^2(\delta) X_{\alpha\alpha} + \sin^2(\delta) X_{\beta\beta},$$
$$X_{bb} = \sin^2(\delta) X_{\alpha\alpha} + \cos^2(\delta) X_{\beta\beta}.$$

In Table 8 these results are marked by ^{a} (for $\delta = 27.83°$) and ^{b} (for $\delta = 26.25°$), respectively.

A third choice for δ is suggested by the close agreement of $X_{\beta\beta}$ in nitromethane and nitrobenzene. If one assumes that $X_{\beta\beta} = 0.304$ MHz also in nitroethylene, $\delta = \measuredangle(\alpha, a) = 25.07°$ is required. The corresponding quadrupole coupling constants are marked by ^{c} in Table 8. The close agreement of $X_{\alpha\alpha}, X_{\beta\beta}, X_{\gamma\gamma}$, which is thus obtained for all three molecules, indicates that the α-principal axis of the ^{14}N coupling tensor might indeed be tilted with respect to the C–N bond direction by up to 3°. Furthermore, the close agreement also indicates that the ^{14}N quadrupole coupling constants observed in nitromethane and in nitrobenzene are typical for the NO_2-group, if bonded to a carbon atom. The local electronic configuration around the ^{14}N nucleus appears to be very similar in this class of molecules. For predictive purposes we therefore propose to use

$X_{\alpha\alpha} = -1.17$ MHz,

$X_{\beta\beta} = +0.30$ MHz,

$X_{\gamma\gamma} = +0.87$ MHz

(with the γ-axis perpendicular to the NO_2-plane and with the α-axis in direction of the bisector of the O–N–O bond angle) as typical values for the ^{14}N quadrupole coupling constants if the NO_2-group is attached to a carbon frame. We reall, however, the strong dependence of the ^{14}N quadrupole coupling constants on the adjacent bond. For instance in the $-O-NO_2$ configuration, if attached to H or CH_3, we have found [3]

$X_{\alpha\alpha} = +1.10$ MHz,

$X_{\beta\beta} = -1.03$ MHz,

$X_{\gamma\gamma} = -0.07$ MHz

as typical values for the ^{14}N quadrupole coupling constants. For both configurations we believe that the ^{14}N quadrupole coupling constants of new molecules, in which the $-NO_2$ or $-O-NO_2$ unit is single bonded to carbon, can be predicted within ± 0.1 MHz if the appropriate set of "typical values" is used.

We now turn to the comparison of the experimental ^{14}N quadrupole coupling constants with ab initio results. For this purpose we did run the Hartree-Fock SCF routine from the Gaussian 88 program package [22] mounted at the University of Kiel CRAY X-MP computer. We tried basis sets of increasing size in

Table 9. r_s-coordinates of the nuclei in nitromethane, taken from Table 7 in [23]. They were used as input data for the Hartree-Fock SCF-calculations.

	a [Å]	b [Å]	c [Å]
C	1.4018	0.0000	0.0000
N	−0.0892	0.0000	0.0000
O1	−0.6500	1.0883	0.0000
O2	−0.6500	−1.0883	0.0000
H1	1.7264	−1.0392	0.0000
H2	1.7264	0.5196	0.9000
H3	1.7264	0.5196	−0.9000

order to get an impression of the basis set dependence of the results. The calculations were carried out only for nitroethylene and nitromethane in order to save computer time, but we believe that the results are fairly representative for nitro-compounds in general. For both molecules we have used the microwave substitution structures as input data (see Table 1 for nitroethylene and Table 9 for nitromethane [23]).

As largest basis we have used the 6-311 G** basis, i.e. a triple zeta valence basis including polarization functions (d-orbitals at C, N, and O and p-orbitals at H). In Table 10 we present the results. We note that the ab initio program calculates the second derivatives of the intramolecular Coulomb potential at the ^{14}N nucleus rather than the quadrupole coupling constants. But the conversion from the second derivatives (typically given in atomic units, a.u.) to the experimental coupling constants (typically given in MHz) is given by

$$X_{gg} = \frac{e^2}{a_0^3} \frac{10^{-6}}{h} Q \left\langle \frac{\partial^2 V}{\partial g^2} \right\rangle \quad (g = a, b, c)$$

or

$$X_{gg} = \left\langle \frac{\partial^2 V}{\partial g^2} \right\rangle_{\text{a.u.}} \cdot Q_{\text{mbarn}} \cdot 0.234973 \text{ MHz} \\ \cdot \text{mbarn}^{-1} \cdot \text{a.u.}^{-1},$$

where a_0 is Bohr's radius, $\langle \partial^2 V/\partial g^2 \rangle$ the vibronic ground state expectation value of the second derivative of the intramolecular Coulomb potential at the position of the ^{14}N nucleus, and where in the lower equation the nuclear quadrupole moment, Q, is measured in mbarn $= 10^{-27}$ cm^2. For the ^{14}N nucleus, Winter and Andrä [24] have determined $Q = 19.3(8)$ mbarn $= 1.93(8) \cdot 10^{-26}$ cm^2. If one used this experimental Q value, the coupling constants calculated from the ab initio field gradients would be far off reality. They are not given in Table 10. Clearly the use of the SCF wavefunctions leads to an error in the electronic contribution to the field gradient.

Table 10. Comparison between the experimental values for the ^{14}N quadrupole coupling constants and the corresponding values calculated from the SCF field gradients for nitroethylene and nitromethane. We note that the SCF-values for the angle $\delta = \measuredangle (\alpha, a)$ ranging between 26.06° and 26.44° are very close to the angle between the a-axis and the bisector of the O–N–O bond angle, 26.25°. In nitromethane the small off-diagonal element, X_{ab}, is averaged to zero by internal rotation. (A 180° rotation of the CH_3-subunit leads to the same absolute value but with opposite sign.) The SCF values were calculated using $Q = 16.8$ mbarn as 'effective ^{14}N quadrupole moment' for the conversion from the SCF field gradients to the experimental coupling constants (see text).

		exp	6-311G**	6-311G	6-31G**	6-31G
Nitroethylene	X_{aa} [MHz]	−0.8887 (18)	−1.7178	−1.5114	−1.7054	−1.5633
	X_{bb} [MHz]	0.0429 (29)	−1.0149	−0.6210	−0.9282	−0.8533
	X_{cc} [MHz]	0.8458 (29)	2.7327	2.1324	2.6337	2.4166
	X_{ab} [MHz]	–	−0.4642	−0.5745	−0.5007	−0.4562
	[°]	–	26.44	26.11	26.09	26.06
Nitromethane	X_{aa} [MHz]	−1.185 (7)	−2.0729	−1.9250	−2.0389	−1.8720
	X_{bb} [MHz]	0.305 (12)	−0.7143	−0.2512	−0.6394	−0.5709
	X_{cc} [MHz]	0.880 (12)	2.7872	2.1763	2.6783	2.4429
	X_{ab} [MHz]	–	0.0181	0.0179	0.0207	0.0216

Table 11. Comparison of the experimental values for the molecular electric dipole moments, molecular electric quadrupole moments, and the anisotropies in the electronic second moments with the corresponding Hartree-Fock SCF results calculated at the structures presented in Tables 1 and 9. For completeness we also give values for the second electronic moments themselves. a) Calculated using $\langle c^2 \rangle = 5.75$ (25) Å^2 from the rule of thumb as additional input (uncertainty estimated). b) Calculated using $\xi_{bulk} = -21.1$ (10) $\cdot 10^{-6}$ erg $\cdot$ G^{-2} $\cdot$ mole^{-1} [19] as additional input (uncertainty estimated). For nitromethane the experimental values are taken from [1].

		exp	6-311G**	6-311G	6-31G**	6-31G
Nitroethylene	μ_a [D]	3.51 (2)	4.497	4.772	4.481	4.887
	μ_b [D]	1.16 (8)	1.431	1.498	1.413	1.532
	Q_{aa} [10^{-26} esu $\cdot$ cm^2]	−0.59 (29)	2.357	2.395	2.347	2.379
	Q_{bb} [10^{-26} esu $\cdot$ cm^2]	0.07 (36)	−1.645	−2.091	−1.583	−2.153
	Q_{cc} [10^{-26} esu $\cdot$ cm^2]	0.52 (46)	−0.712	−0.304	−0.764	−0.226
	$\langle a^2 - b^2 \rangle$ [Å^2]	36.55 (7)	35.91	35.84	35.92	35.83
	$\langle b^2 - c^2 \rangle$ [Å^2]	23.58 (9)	23.65	23.77	23.64	23.79
	$\langle c^2 - a^2 \rangle$ [Å^2]	−60.14 (8)	−59.56	−59.61	−59.56	−59.62
	$\langle a^2 \rangle$ [Å^2]	65.89 (26)[a]	65.60	65.72	65.55	65.70
	$\langle b^2 \rangle$ [Å^2]	29.33 (26)[a]	29.69	29.88	29.63	29.87
	$\langle c^2 \rangle$ [Å^2]	5.75 (25)[a]	6.04	6.11	5.99	6.08
Nitromethane	μ_a [D]	3.46 (2)	4.240	4.484	4.187	4.557
	μ_b [D]	–	−0.013	−0.004	−0.016	−0.007
	Q_{aa} [10^{-26} esu $\cdot$ cm^2]	2.40 (15)	3.070	3.349	3.087	3.438
	Q_{bb} [10^{-26} esu $\cdot$ cm^2]	−4.58 (16)	−5.769	−6.413	−5.597	−6.520
	Q_{cc} [10^{-26} esu $\cdot$ cm^2]	2.18 (19)	2.699	3.064	2.510	3.082
	$\langle a^2 - b^2 \rangle$ [Å^2]	6.01 (8)	5.75	5.62	5.77	5.59
	$\langle b^2 - c^2 \rangle$ [Å^2]	19.89 (6)	20.12	20.26	20.08	20.28
	$\langle c^2 - a^2 \rangle$ [Å^2]	−25.90 (6)	−25.87	−25.88	−25.85	−25.88
	$\langle a^2 \rangle$ [Å^2]	32.01 (13)[b]	31.96	32.02	31.94	32.03
	$\langle b^2 \rangle$ [Å^2]	26.00 (13)[b]	26.21	26.40	26.17	26.44
	$\langle c^2 \rangle$ [Å^2]	6.11 (12)[b]	6.09	6.14	6.09	6.15

Now, since the values of the second derivatives are dominated by the contribution of the close electronic environment of the ^{14}N nucleus – the contributions of the other nuclei and "their" electrons largely cancel, irrespective of the quality of the electronic wavefunctions – one can try to compensate the local errors in the wavefunction by using Q as a basis set dependent scaling factor. Proceeding like that in a systematic study of imines, Krause from our group got satisfactory results with $Q = 16.8$ mbarn as scaling factor for the imine-nitrogen and the 6-311 G** basis [25]. With this "pseudo quadrupole moment", the quadrupole

coupling tensors of a whole set of imines could be calculated from their 6-311 G** field gradients within better than ± 90 kHz!

We have therefore tried Krause's "effective" ^{14}N quadrupole moment, $Q = 16.8$ mbarn, also for the nitro compounds. The agreement with the experimental values is still very poor. Also one single calibration factor is clearly insufficient. Part of the discrepancy between the experimental and the calculated values might be caused by our neglection of zero point vibrations. But from our experience with formaldoxime [10] we do not believe that vibrational corrections would greatly reduce the discrepancies. We further find it interesting to note that inclusion of polarization functions as indicated by the asterisks (**) worsens the agreement with experiment, while the change from the 6-31 G basis to the slightly more flexible 6-311 G basis has only comparatively little effect. In our opinion this indicates that electron correlation has to be taken into account if better agreement between the ab initio results and the experimental quadrupole coupling constants is required.

Finally we turn to the comparison between the experimental values for the electronic dipole moments, the molecular electric quadrupole moments and for the anisotropies in the second electronic moments with the corresponding SCF-values. The values for the latter quantities always turn out to be close to the corresponding differences in the nuclear second moments (see above). The data are presented in Table 11. These molecular parameters are more dependent on the quality of the electron wavefunctions in the outer regions of the molecule and here, quite in contrast to the observation for the field gradients, inclusion of polarization functions clearly improves the agreement with the experimental values. But even with the 6-311G** basis the discrepancies between the RHF-SCF results and the experimental value are still large. This came as a surprise to us, since the RHF-SCF wavefunctions calculated with the 6-311G** basis used here did quite well for the imines studied by Krause [25].

Obviously, from the point of view of quantum chemistry the nitro compounds, even smaller ones, appear to qualify as "difficult" molecules. Larger and better basis sets and certainly better account for electron correlation will be required if one wants to get better agreement with reality. The microwave results for the structures, the electric dipole moments, the molecular electric quadrupole moments, and the ^{14}N nuclear quadrupole coupling constants, the two latter quantities being the subject of the present investigations, provide critical test data for such more sophisticated calculations.

[1] L. Engelbrecht, Ph.D. thesis, Kiel 1975.
[2] L. Albinus, J. Spieckermann, and D. H. Sutter, J. Mol. Spectroscop. **133**, 128 (1989).
[3] J. Spieckermann and D. H. Sutter, Z. Naturforsch. **44a**, 1087 (1989).
[4] T. G. Schmalz, C. L. Norris, and W. H. Flygare, J. Amer. Chem. Soc. **95**, 7961 (1973).
[5] D. H. Sutter and W. H. Flygare, Top. Curr. Chem. **63**, 89 (1976).
[6] H. D. Hess, A. Bauder, and Hs. H. Günthard, J. Mol. Spectrosc. **22**, 208 (1967).
[7] P. Nösberger, A. Bauder, and Hs. H. Günthard, Chem. Phys. **8**, 245 (1975).
[8] H. Wieland and E. Sakellarios, Ber. Dtsch. Chem. Ges. **52**, 898 (1919).
[9] D. Sutter, Z. Naturforsch. **26a**, 1644 (1971).
[10] A. Klesing and D. H. Sutter, Z. Naturforsch. **45a**, 817 (1990).
[11] W. Gordy and R. L. Cook, Microwave Molecular Spectra, 3rd ed., John Wiley & Sons, New York 1984, Eqs. 7.3 and 9.75.
[12] K. F. Dössel and D. H. Sutter, Z. Naturforsch. **32a**, 1444 (1977).
[13] G. C. Wick, Z. Physik **85**, 25 (1933).
[14] J. R. Eshbach and M. W. P. Strandberg, Phys. Rev. **85**, 24 (1952).
[15] J. H. Van Vleck, The Theory of Electric and Magnetic Susceptibilities, Oxford University Press, 1932.
[16] W. Hüttner, M.-K. Lo, and W. H. Flygare, J. Chem. Phys. **48**, 1206 (1968).

[17] D. H. Sutter and W. H. Flygare, J. Amer. Chem. Soc. **91,** 6895 (1969).

[18] W. Haberditzl, S. B. Deutsche Akad. Wiss. Berlin, Chem. Geol. Biol., 1964, No. 2.

[19] R. C. West, Ed., CRC Handbook of Chemistry and Physics, 65th ed., Tab. E-115, CRC Press Inc., Boca Raton 1984.

[20] A. P. Cox, S. Waring, and K. Morgenstern, Nature London **229,** 22 (1971).

[21] N. Heineking, private communication.

[22] M. J. Frisch, M. Head-Gordon, H. B. Schlegel, K. Raghavachari, J. S. Binkley, C. Gonzales, D. J. Defrees, D. J. Fox, R. A. Whiteside, R. Seeger, C. F. Melius, J. Baker, R. L. Martin, L. R. Kahn, J. J. P. Stewart, E. M. Fluder, S. Topiol, and J. A. Pople, Gaussian Inc., Pittsburgh.

[23] A. P. Cox and S. Waring, J. Chem. Soc. Faraday Trans. II **68,** 1060 (1972).

[24] H. Winter and H. J. Andrä, Phys. Rev. A **21,** 581 (1980).

[25] H. Krause, private communication, manuscript in preparation.